A new series of mixed-metal cuprates in the T′ structure: $Nd_{2-x-y}A_xCe_yCuO_{4-\delta}$ (A^{II} = Mg and Ca)

S. Wang, J. D. Carpenter, S.-J. Hwu*
Department of Chemistry, P.O. Box 1892, Rice University, Houston, TX 77251 (USA)

R. Sauerbrey
Department of Electrical and Computer Engineering, Rice University, Houston, TX 77251 (USA)

J. T. Vaughey, K. R. Poeppelmeier
Department of Chemistry, Northwestern University, Evanston, IL 60208 (USA)

S. N. Song and J. B. Ketterson
Department of Physics and Astronomy, Northwestern University, Evanston, IL 60208 (USA)

(Received December 23, 1991)

Abstract

We report the synthesis of a new series of layered copper oxide compounds, $Nd_{2-x-y}A_xCe_yCuO_{4-\delta}$ (A^{II} = Mg and Ca), which are isostructural with the T′-phase of the superconducting, n-type $Nd_{2-x}Ce_xCuO_{4-\delta}$. An extended solid solubility range, $x+y \leqslant 0.60$, is observed. The as-prepared air-quenched samples show semiconducting behavior. These newly prepared compounds raise further questions about electron-doped superconductivity in the cuprate oxides.

Introduction

Since the discovery [1] of n-type high transition-temperature (high T_c) superconductivity in cerium-doped $Ln_{2-x}Ce_xCuO_4$ (Ln = Pr, Nd and Sm) compounds, the effort to understand the fundamental parameters that describe electron-type superconductivity [2] has been two-fold. Synthetically, the substitution of fluorine for oxygen [3] in Nd_2CuO_4 has been employed as an alternative route for achieving a reduction of copper, electron conductivity and superconductivity ($T_c \approx 27$ K). Chemical substitutions by tetravalent cations [4, 5] demonstrate that the superconductivity appears to be associated with electrons in the CuO_2 planes, which are donated by tetravalent (or intermediate valent, +3 and +4) Ce and Th when substituted for trivalent lanthanide cations, e.g. $Eu_{2-x}Ce_xCuO_{4-\delta}$ and $(Nd, Pr)_{2-x}Th_xCuO_{4-\delta}$. Experimental evidence from both photoemission spectroscopy [6] and X-ray absorption spectroscopy (XAS) [7] have confirmed that the system is indeed doped with electrtons. Theoretically, the local density functional energy band calculations [8] of T′-$Nd_{2-x}Ce_xCuO_{4-\delta}$ reveal that the electronic structure of this electron-doped superconductor near the Fermi level (E_F) is similar to the hole-doped superconductors. The unique feature of the band structure appears to be the additional O(2) p-band, lying just below E_F, that has resulted from the interaction of p_z–p_z orbitals from vertical O(2)–O(1)–O(2)–O(1) chains (see structure description below).

The Ce-doped superconductors adopt the Nd_2CuO_4 structure (T′-phase, as shown in Fig. 1) which is composed of a metal framework similar to that of K_2NiF_4. In the T′ structure the Cu is coordinated to four oxygens, O(1) atoms, in a square planar geometry. In contrast to La_2CuO_4 (T-phase), the O(2) atoms are in a totally different position than the apical oxygen of Cu. They share the same in-plane symmetry as the O(1) atoms and also connect the O(1) atoms along the z direction perpendicular to the Cu–O(1) plane. In the T′-phase, the A-site cation (Nd in this case) has a coordination number of eight, which is the same as that found in $YBa_2Cu_3O_7$, but less than nine as seen in La_2CuO_4 and $La_{2-x}Sr_xCuO_4$ (T-phase). It is interesting to note that the structure of the Sr-codoped n-type $Nd_{2-x-y}Sr_xCe_yCuO_{4-\delta}$ superconductors ($T_c \approx 28$ K) [9–11] no longer retains the T′-structure, but rather they possess the T*-structure which has the same metal

*Author to whom correspondence should be addressed.

0020-1693/92/$5.00

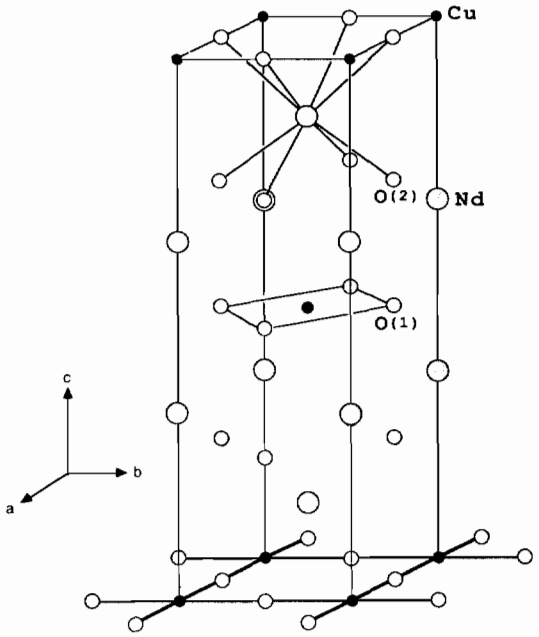

Fig. 1. A schematic drawing of the structure of T′-Nd_2CuO_4.

framework but a different oxygen arrangement. Its structure can be described as a combination of T-phase (e.g. CuO_6 octahedral in $La_{2-x}Sr_xCuO_{4-\delta}$) and T′-phase (e.g. CuO_4 square planar in $Nd_{2-x}Ce_xCuO_{4-\delta}$), giving rise to a square pyramidal coordination at the Cu sites; e.g. CuO_5. Furthermore, ordering of the cations, Nd(Ce) versus Nd(Sr), is found in the structural fragments of T′ versus T, respectively. However, the factors that govern the phase formation of T, T* or T′ are not totally understood.

In this paper we describe the synthesis, crystal structure and conductivity of divalent cation-doped T′-$Nd_{2-x-y}A_xCe_yCuO_z$ (A^{II} = Mg and Ca). We demonstrate that the relative cation sizes of Mg^{2+} and Ca^{2+} (including Ce^{4+}) versus Nd^{3+} may be responsible for retaining the T′-structure. Superconductivity appears to be introduced by Ce^{4+} doping in the compounds of $Nd_{2-x}Ce_xCuO_{4-\delta}$ ($\delta \approx 0.04$) [1] but does not exist in the current systems due to an appreciable amount of oxygen deficiency.

Experimental

Polycrystalline samples of $Nd_{2-x-y}A_xCe_yCuO_z$ (A^{II} = Mg and Ca) were prepared by the solid state reaction of Aldrich cupric oxide (99.999%), magnesium oxide (99.99%), calcium carbonate (99.995%), cerium oxide (99.9%) and neodymium oxide (99.9%). Powders were ground with a mortar and pestle and calcined in air three times (12 h each time) with intermittent grindings at temperatures ranging from 950 to 1000 °C. The dark black samples were pressed into pellets before continuing the reaction at higher temperatures, e.g. 1000–1100 °C. The products were reground and repelletized twice. Thermogravimetric studies (with a DuPont 9900 Thermal Analysis System) were performed in a hydrogen atmosphere to determine the oxygen composition.

Disc-shaped specimens, 12 mm in diameter and 1 mm thick, were isostatically pressed at 12 Kbar at room temperature for resistivity measurements. The pellets were sintered at 1000–1100 °C and quenched in air. Discs were checked for metallic behavior using a two-probe voltmeter from room temperature down to liquid nitrogen temperature. Selected discs were cut into rectangular specimens with cross sections of 3×7 mm and four leads were attached with silver paint for 4-point resistivity measurements.

X-ray diffraction (XRD) measurements were carried out on pelletized polycrystalline samples. XRD powder patterns were recorded on a Philips PW1840 diffractometer with Cu Kα radiation and a Ni filter. National Bureau of Standards (NBS) silicon was used for an internal standard. The XRD powder patterns ($20 \leqslant 2\theta \leqslant 60°$) were indexed and refined by the least-squares program LATT [12] with constraint to the tetragonal crystal system. The refined lattice parameters of observed XRD powder patterns with 9–12 reflections are tabulated in Table 1.

Results and discussion

The current research was motivated by the following questions: (i) what is required for a structure to retain a T′-phase and (ii) what happens to the superconductivity when the degree of orbital overlaps between oxygens p_z–p_z and Cu–O(1) dpσ bands varies because of a reduction in the c-axis dimension? The latter may be achieved by pressure* or, alternatively, by substituting smaller cations for Nd^{3+}. For this purpose, two relatively small (compared to Sr^{2+}) divalent cations, Mg^{2+} and Ca^{2+}, were chosen to substitute for Nd^{3+} in the following Ce-codoped systems: $Nd_{2-x-y}Mg_xCe_yCuO_{4-\delta}$ (system A, $y = x - 0.20$), $Nd_{2-x-y}Ca_xCe_yCuO_{4-\delta}$ (system B, $y = x - 0.20$), and $Nd_{1.80-y}Ca_{0.20}Ce_yCuO_{4-\delta}$ (system C, $y = 0.05$–0.25). Systems A and B were prepared in an attempt to achieve an isoelectronic substitution (see later discussion). In system C, the effect of copper reduction on superconductivity was investigated by re-

*Pressure-dependent electrical resistivity measurements reveal an increase of T_c with applied pressure for $Nd_{1.85}Ce_{0.15}CuO_{4-\delta}$ ($\delta = 0.02$) at a rate of $\sim dT_c/dp \approx 0.025$ K/Kbar, see ref. 14.

TABLE 1. Cell parameters and TGA results of T′-$Nd_{2-x-y}A_xCe_yCuO_z$ (A^{II} = Mg, Ca)

Compositions	a (Å)	c (Å)	c/a	z[a]
System A ($y=x-0.2$)				
$Nd_{1.80}Mg_{0.20}CuO_z$	3.9446(7)	12.181(2)	3.09	3.80
$Nd_{1.70}Mg_{0.25}Ce_{0.05}CuO_z$	3.947(2)	12.137(6)	3.08	3.72
$Nd_{1.60}Mg_{0.30}Ce_{0.10}CuO_z$	3.951(2)	12.119(5)	3.07	3.70
$Nd_{1.50}Mg_{0.35}Ce_{0.15}CuO_z$	3.951(2)	12.082(6)	3.06	3.67
'$Nd_{1.40}Mg_{0.40}Ce_{0.20}CuO_z$'	3.952(2)	12.072(6)	3.06	NA[b]
'$Nd_{1.30}Mg_{0.45}Ce_{0.25}CuO_z$'	3.9497(9)	12.057(4)	3.05	NA[b]
System B ($y=x-0.2$)				
$Nd_{1.80}Ca_{0.20}CuO_z$	3.944(1)	12.162(4)	3.08	4.06
$Nd_{1.70}Ca_{0.25}Ce_{0.05}CuO_z$	3.9445(6)	12.145(2)	3.08	4.00
$Nd_{1.60}Ca_{0.30}Ce_{0.10}CuO_z$	3.946(2)	12.104(8)	3.07	3.84
$Nd_{1.50}Ca_{0.35}Ce_{0.15}CuO_z$	3.944(2)	12.082(6)	3.06	3.84
$Nd_{1.45}Ca_{0.37}Ce_{0.18}CuO_z$	3.946(1)	12.073(5)	3.06	3.78
$Nd_{1.40}Ca_{0.40}Ce_{0.20}CuO_z$	3.946(1)	12.052(4)	3.05	3.74
'$Nd_{1.30}Ca_{0.45}Ce_{0.25}CuO_z$'	3.948(1)	12.062(4)	3.06	NA[b]
System C ($x=0.20$, $y=0.05$–0.25)				
$Nd_{1.75}Ca_{0.20}Ce_{0.05}CuO_z$	3.9468(8)	12.148(3)	3.08	3.87
$Nd_{1.70}Ca_{0.20}Ce_{0.10}CuO_z$	3.946(1)	12.118(4)	3.07	3.88
$Nd_{1.65}Ca_{0.20}Ce_{0.15}CuO_z$	3.9429(9)	12.077(3)	3.06	3.91
$Nd_{1.60}Ca_{0.20}Ce_{0.20}CuO_z$	3.9485(8)	12.070(5)	3.06	3.91
'$Nd_{1.55}Ca_{0.20}Ce_{0.25}CuO_z$'	3.9439(9)	12.064(3)	3.06	NA[b]
Nd_2CuO_4	3.9453(6)	12.174(2)	3.09	3.95
$Nd_{1.85}Ce_{0.15}CuO_{3.93}$[c]	3.946	12.081	3.06	
$Nd_{1.85}Ce_{0.15}CuO_z$	3.954(1)	12.092(5)	3.06	3.95

[a]The oxygen stoichiometries (±0.02) are calculated based upon the TGA results. [b]Not available. The reaction product is not a single phase (see text). [c]Ref. 13.

ducing the oxidation state of the copper cation through the substitution of trivalent Nd^{3+} cations with tetravalent Ce^{4+} cations.

All magnesium- and calcium-codoped compounds adopt the Nd_2CuO_4 structure (T′-phase) according to the XRD patterns. In Fig. 2 a typical XRD pattern of Mg-doped $Nd_{2.00-x}Mg_xCuO_{4-\delta}$ ($x=0.20$ and $\delta=0.24$) is shown and compared with that of T′-Nd_2CuO_4 [15]. The 103 (or 013) and 110 reflections, that show a very small separation around 32° in 2θ, are indicative peaks

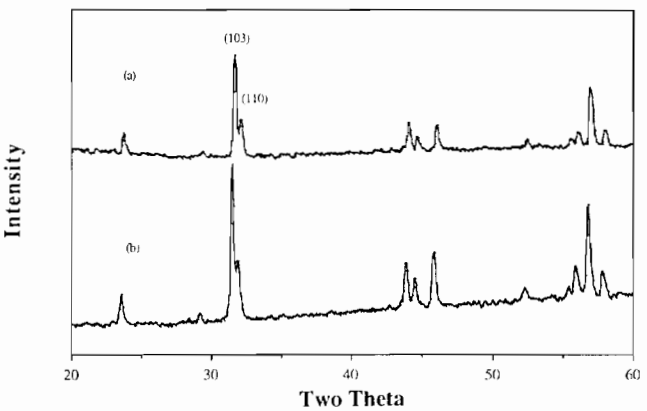

Fig. 2. Powder X-ray diffraction patterns of (a) Nd_2CuO_4 (T′-phase) and (b) T′-$Nd_{1.80}Mg_{0.20}CuO_{3.76}$.

of the T′-phase. No evidence shows that the divalent cations, Mg and Ca in this case, are ordered.

As reported in Table 1, a change in the cell parameters is observed. This phenomenon is expected, since the size of the Nd^{3+} cation is different from that of Mg^{2+}, Ca^{2+} and Ce^{4+}. The Shannon [16] crystal radii for eight-coordinated Nd^{3+}, Ce^{4+}, Ca^{2+} and Mg^{2+} ions are 1.249, 1.11, 1.26 and 1.03 Å, respectively. (The calculated radius for the magnesium cation is comparable with that observed in synthetic pyrope ($Mg_3Al_2Si_3O_{12}$) [17]*.) This cation size effect can be readily seen from the merging of the 103 (or 013) and 110 reflections, as shown in Fig. 3. For example, these two diffraction peaks in the $Nd_{2-x-y}Mg_xCe_yCuO_4$ XRD patterns move toward each other as the total substituents ($x+y$) increase from 0.2 to 0.6. A closer examination of the peak positions revealed that the (103) peak moves to higher angles and the (110) peak moves to slightly lower angles, indicating a contraction of the c axis and an expansion of the a axis as the concentration of the dopant increases. For both magnesium and

*The Mg–O bond distances in a distorted MgO_8 cube are 2.198 and 2.343 Å. The eight coordinated Mg radii, resulting from subtracting the four-coordinated O^{2-} crystal radius (1.24 Å) are 0.96 and 1.10 Å.

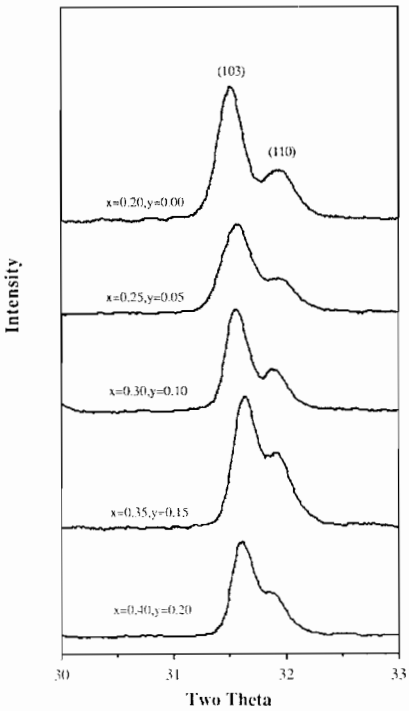

Fig. 3. Sections of X-ray diffraction patterns showing the (103) and the (110) reflections of $Nd_{2-x-y}Mg_xCe_yCuO_{4-\delta}$.

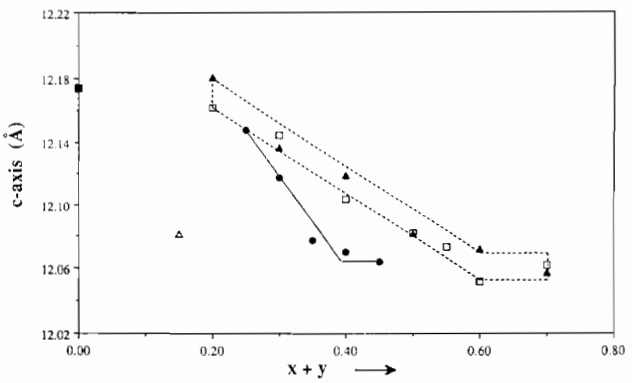

Fig. 4. Values of lattice dimensions vs. total amount of dopant $(x+y)$ of $Nd_{2-x-y}A_xCe_yCuO_{4-\delta}$: system A ($A^{II}$=Mg, ▲), system B ($A^{II}$=Ca, □), system C (●) and, for comparison, lattice parameters of Nd_2CuO_4 (■) and $Nd_{1.85}Ce_{0.15}CuO_4$ (△).

calcium doped systems, the c/a ratios range from 3.05 to 3.09 (see Table 1), which is also a characteristic of the T′-phase.

In Fig. 4, a linear relationship between c and $(x+y)$ indicates that the cation substitution in the $Nd_{2-x-y}A_xCe_yCuO_4$ compounds is successful. The solubility limits (x_c) for systems A (Mg-doped), B (Ca-doped) and C are 0.60, 0.60 and 0.35, respectively, according to Vegard's Law. These values are all significantly higher than that of Ce-doped $Nd_{2-x}Ce_xCuO_4$ ($x_c=0.2$) [13]. The c lattice parameter decreases as the concentration of the dopant increases. Expectedly, the unit cell volume decreases with increasing $(x+y)$. The contraction in c is thought to be primarily due to the presence of the smaller Ce^{4+} cation. This effect is more profoundly shown in system C. However, the change in the cell dimensions is rather complicated. It is more likely attributed to the combination of the size of the substituent, the oxidation state of the copper atom and the oxygen deficiency (δ).

Let us first look at the so called 'isoelectronic' systems A and B, where the copper oxidation state presumably stays the same if $\delta=0$. For each divalent magnesium (Mg^{2+}) or calcium (Ca^{2+}) cation substituted for a trivalent neodymium (Nd^{3+}), a tetravalent cerium (Ce^{4+}) cation was co-substituted to keep the charge balanced. In $Nd_{1.80}A_{0.20}CuO_z$ systems (A = Mg and Ca), the c axis of Mg^{2+}-doped compounds is larger than that of the calcium analogue, e.g. 12.181(2) versus 12.162(4) Å, respectively. This comparison in c leads to a result which is the opposite of what one would expect when decreasing the cation size, e.g. Ca > Mg. Further studies indicate that this opposite trend may be associated with the oxygen stoichiometry (z), e.g. Ca (4.06) versus Mg (3.76). While the charge of electropositive divalent cations (Ca^{2+} and Mg^{2+}) remains unchanged, the reduction due to less oxygen stoichiometry may occur on the copper site. The reducing electrons, which presumably fill the Cu–O(1) dpσ antibonding orbitals, give rise to the longer c axis. It is noted that the possibility of incorporation of Mg^{2+} cations in the copper sites, which would give rise to the above described opposite trend, cannot be totally ruled out. However, careful XRD powder pattern examinations show no sign of a second phase in the solid solution region.

The thermogravimetric analysis (TGA) reveals that these compounds are highly oxygen deficient (Table 1). This phenomenon becomes more obvious in the solid solution regions with higher levels of dopant concentrations. In $Nd_{1.50}Mg_{0.35}Ce_{0.15}CuO_{3.67}$, for example, extensive oxygen deficiency leads to a formal oxidation state of copper which is reduced to as low as 1.54. It is also noted that $Nd_{1.8}Ca_{0.2}CuO_4$ shows no oxygen defects (within experimental error by TGA) while $Nd_{1.8}Mg_{0.2}CuO_{4-\delta}$ ($\delta=0.24$) shows a significant oxygen deficiency. This may be attributed to the small size cation effect which decreases the oxygen coordination number with respect to A-site cations. In any case, based only on powder XRD patterns there is no structural evidence to show that the oxygen vacancies are ordered. However more complete characterization with HREM is required.

The TGA results from system C are interesting in a sense that the oxygen stoichiometry seemingly increases as the concentration of the Ce dopant (y) goes higher, see Table 1. Thus the calculated formal oxidation

state of copper ranges in an increasing order from 1.82 to 1.89. In increasing the Ce-dopant level, the systematic trend in decreasing *c*-lattice parameter is still evident. This suggests that the dominating factors in determining the *c*-axis dimension are primarily the size of the substituent and, to a lesser extent, oxygen vacancies.

The temperature dependent resistivity was measured for the title compounds, $Nd_{2-x-y}A_xCe_yCuO_4$. Although they all show semiconducting behavior, doping with Mg^{2+} and Ce^{4+} ions improves the conductivity remarkably when compared to the undoped compound, Nd_2CuO_4 [11, 18]. Post oxygen annealing in an ambient atmosphere does not increase the oxygen content nor change the bulk conductivity significantly. While the results are preliminary, our findings do reflect two points: first, doping with smaller cations improves the conductivity by a factor of 1000 and second, high pressure oxygen annealing may help in decreasing oxygen vacancies, possibly favoring superconductivity. It is known that high pressure oxygen produces bulk superconductivity in some Sr-doped phases [10, 19].

In conclusion, all of these newly prepared compounds, $Nd_{2-x-y}M_xCe_yCuO_{4-\delta}$ (M = Mg and Ca), crystallize in the T′-structure as opposed to Sr-doped compounds which form the T*-phase. This research demonstrates that the size of the A-site cations is responsible for retaining the T′-phase. It is not known, however, whether the lack of superconductivity is associated with the difference in the crystal structures (T′ versus T*) or to the extended oxygen vacancies. Nevertheless, co-doping with both divalent and tetravalent cations extends the solubility limit (0.60 for the Mg^{2+}- and Ca^{2+}-doped compounds), and, moreover, significantly improves the conductivity of the T′-phase. The small cations affect on the resistivity, coupled with the large oxygen deficiency indicates that high pressure oxygen annealing studies need further investigation in order to understand the T_c with respect to the carrier concentration and crystal structure.

Acknowledgements

This work was supported by the Robert A. Welch Foundation and a Rice University startup grant (S.-J.H.) and by the Science and Technology Center for Superconductivity at Northwestern University (Grant NSF-DMR-8809854). The authors are indebted to Ms M. V. Deaton for helping with the sample preparation.

References

1 Y. Tokura, H. Takagi and S. Uchida, *Nature (London), 337* (1989) 345.
2 V. J. Emery, *Nature (London), 337* (1989) 306.
3 A. C. W. P. James, S. M. Zahurak and D. W. Murphy, *Nature (London), 338* (1989) 240.
4 J. T. Markert and M. B. Maple, *Solid State Commun., 70* (1989) 145.
5 J. T. Markert, E. A. Early, T. Bjørnholm, S. Ghamaty, B. W. Lee, J. J. Neumeier, R. D. Price, C. L. Seaman and M. B. Maple, *Physica C, 158* (1989) 178.
6 A. Fujimori, Y. Tokura, H. Eisake, H. Takagi, S. Uchida and E. Takayama-Muromachi, *Phys. Rev. B, 42* (1990) 325.
7 E. E. Alp, S. M. Mini, M. Ramanathan, B. Dabrowski, D. R. Richards and D. G. Hinks, *Phys. Rev. B, 40* (1989) 2617.
8 S. Massidda, N. Hamada, J. Yu and A. J. Freeman, *Physica C, 157* (1989) 571.
9 J. Akimitsu, S. Suzuki, M. Watanabe and H. Sawa, *Jpn. J. Appl. Phys., 27* (1988) L1859.
10 E. Takayama-Muromachi, Y. Matsui, Y. Uchida, F. Izumi, M. Onoda and K. Kato, *Jpn. J. Appl. Phys., 27* (1988) L2283.
11 H. Sawa, S. Suzuki, M. Watanabe, J. Akimitsu, H. Matsubara, H. Watabe, S.-I. Uchida, K. Kohusho, H. Asano, F. Izumi and E. Takayama-Muromachi, *Nature (London), 337* (1989) 347.
12 F. Takusagawa, *LATT,* Ames Laboratory, Iowa State University, Ames, IA, 1981, unpublished research.
13 T. C. Huang, E. Moran, A. I. Nazzal and J. B. Torrance, *Physica C, 158* (1989) 148.
14 J. T. Markert, E. A. Early, T. Bjørnholm, S. Ghamaty, W. B. Lee, J. J. Neumeier, R. D. Price, C. L. Seaman and M. B. Maple, *Physica C, 158* (1989) 178.
15 No. 24-777, Joint Committee on Powder Diffraction Standards, Swarthmore, PA.
16 R. D. Shannon, *Acta Crystallogr., Sect. A, 32* (1976) 751.
17 G. V. Gibbs and J. V. Smith, *Am. Mineral., 50* (1965) 2023.
18 P. Ganguly and C. N. R. Rao, *Mater. Res. Bull., 8* (1973) 405.
19 S.-W. Cheong, Z. Fisk, J. D. Thompson and R. B. Schwarz, *Physica C, 159* (1989) 407.